European Journal of Pharmacology 798 (2017) 129–136

Contents lists available at ScienceDirect

European Journal of Pharmacology

journal homepage: www.elsevier.com/locate/ejphar

Full length article

Loop-F of the α-subunit determines the pharmacologic profile of novel competitive inhibitors of $GABA_A$ receptors

Balázs Mihalik[a], Adrienn Pálvölgyi[a], Ferenc Bogár[c], Katalin Megyeri[a], István Ling[b], József Barkóczy[b], Ferenc Bartha[d], Tamás A. Martinek[e], István Gacsályi[a], Ferenc A. Antoni[a,*]

[a] Division of Preclinical Research, Egis Pharmaceuticals PLC, Hungary
[b] Chemical Research Division, Egis Pharmaceuticals PLC, Budapest, Hungary
[c] MTA-SZTE Supramolecular and Nanostructured Materials Research Group of HAS, University of Szeged, Hungary
[d] Department of Medical Chemistry, University of Szeged, Hungary
[e] Institute of Pharmaceutical Analysis, SZTE-MTA Lendület Foldamer Research Group, University of Szeged, Szeged, Hungary

ARTICLE INFO

Keywords:
GABA
$GABA_A$ antagonists
Molecular modelling
Loop-F
Extrasynaptic receptors
Nootropic agents

ABSTRACT

The neurotransmitter γ-amino butyric acid (GABA) has a fundamental role in CNS function and ionotropic ($GABA_A$) receptors that mediate many of the actions of GABA are important therapeutic targets. This study reports the mechanism of action of novel $GABA_A$ antagonists based on a tricyclic oxazolo-2,3-benzodiazepine scaffold. These compounds are orthosteric antagonists of GABA on heteropentameric $GABA_A$ receptors of αxβ2γ2 configuration expressed in HEK293 cells. *In silico* modelling predicted that the test compounds docked in the GABA binding-pocket and would interact with amino-acid residues in the α- and β-subunit interface that are known to be important for the binding of GABA. Intriguingly, optimal docking also required an interaction with the non-conserved amino-terminal segment of Loop-F of the α–subunit. Testing of a compound with altered regiochemistry of the oxazolone moiety supported the model with respect to the conserved GABA-interacting residues *in vitro* as well as *in vivo*. The prediction regarding loop-F was examined by replacing the amino-terminal variable segment of loop-F of the α5-subunit with the corresponding residues in the α1- and α2-subunits. When tested with the novel inhibitors, the receptors formed by the modified α5-subunits displayed the pharmacologic phenotype of the source of loop-F. In summary, these data show that the variable amino-terminal segment of loop-F of the α-subunit determines the pharmacologic selectivity of the novel tricyclic inhibitors of $GABA_A$ receptors.

1. Introduction

Gamma-aminobutyric acid (GABA) is a fundamentally important neurotransmitter in the CNS (Klausberger and Somogyi, 2008; Walker, 1983). Ionotropic ($GABA_A$) receptors for GABA constitute a subfamily of Cys-loop, ligand-gated ion-channels (CLIG) assembled from a repertory of 19 genes (Barnard et al., 1988; Miller and Smart, 2010; Olsen and Sieghart, 2008; Rudolph and Möhler, 2014). Each receptor consists of five membrane-spanning protein subunits lining a central pore that is highly selective for Cl^- (Barnard et al., 1988; Miller and Smart, 2010; Olsen and Sieghart, 2008; Rudolph and Möhler, 2014). The predominant subunit configuration of neuronal $GABA_A$ receptors is 2α+2β+1γ, i.e. heteropentameric. The GABA ligand-binding pocket is formed at the interface of the extracellular domains of the α and β subunits. Whilst all three subunits are encoded by distinct gene subfamilies, it is thought that the bulk of functional receptor isoforms consist of identical α and β subunits (McKernan and Whiting, 1996). Evidence for naturally occurring "hetero-alpha" $GABA_AR$ complexes has been also published (Araujo et al., 1999; McKernan and Whiting, 1996; Nusser et al., 1998; Pollard et al., 1995). However, the biologic and potential pharmacologic significance of hetero-alpha $GABA_ARs$ remains unclear.

Ionotropic $GABA_A$ receptors are the targets of several types of drugs including barbiturates, benzodiazepines and halogenated inhalational anaesthetics (Olsen and Sieghart, 2008; Rudolph and Möhler, 2014). Whilst therapeutically highly important in a variety of clinical conditions, the use of these drugs is complicated by prominent unwanted side-effects. Thus, considerable effort has been made to develop compounds that would selectively target $GABA_A$ receptor isoforms. The vast majority of the selective compounds developed in the past 20 years were allosteric modulators at the benzodiazepine site (Atack, 2011a; Olsen and Sieghart, 2008; Skolnick, 2012; Wikipedia, 2015).

* Correspondence to: Center for Integrative Physiology, Deanery of Biomedical Sciences, University of Edinburgh, 15 George Sq, Edinburgh EH8 9XD, Scotland, U.K.
E-mail addresses: franzantoni@gmail.com, ferenc.antoni@ed.ac.uk (F.A. Antoni).

http://dx.doi.org/10.1016/j.ejphar.2017.01.033
Received 2 November 2016; Received in revised form 25 January 2017; Accepted 25 January 2017
Available online 31 January 2017
0014-2999/

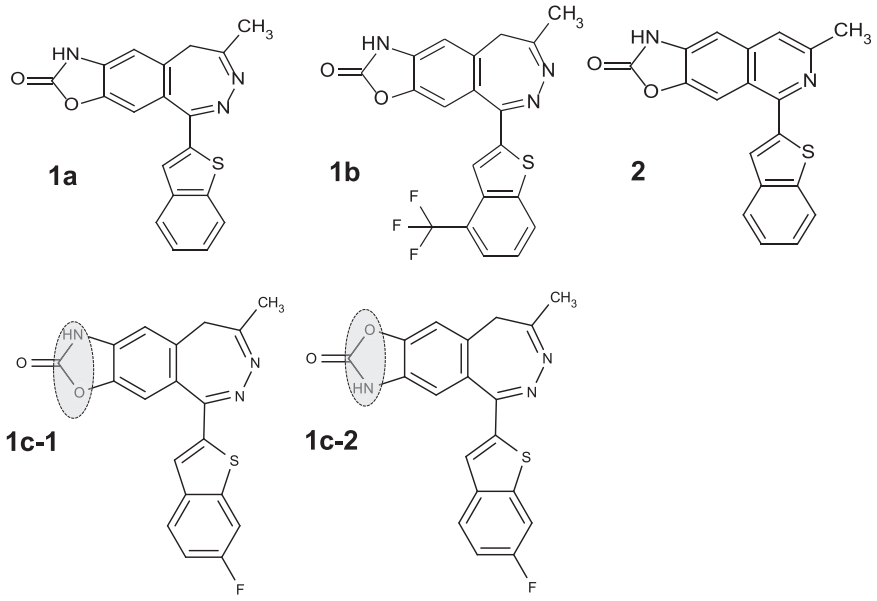

Fig. 1. The test compounds used in this study.

However, the clinical development of all of these drugs, bar basmisanil, has been stopped.

Previously, we reported the chemical synthesis and partial biologic characterization of a family of tricyclic compounds based on an oxazolo-2,3 benzodiazepine scaffold (Ling et al., 2015). The compounds are orthosteric inhibitors of GABA binding at the β–α subunit interface. In some cases this property is paired with inhibition of channel opening induced by etomidate, which is similar to the profile of the GABA antagonist, bicuculline (Ueno et al., 1997). However, in contrast to bicuculline, which is a non-selective blocker of all $GABA_A$ receptor isoforms, some of the novel tricyclic compounds showed considerable isoform selectivity. For instance, compound **1b** (Fig. 1) appears to be a selective blocker of extra-synaptic α5-$GABA_A$Rs (Ling et al., 2015).

The present study investigated the structural determinants of the selectivity of the novel tricyclic $GABA_A$ inhibitors by *in silico* modelling, followed by testing of the predictions of the model by *in vitro* and *in vivo* bioassays. The results confirm previous findings (Ling et al., 2015) that the novel tricyclic antagonists dock in the GABA-binding pocket. Importantly, and in contrast to GABA agonists, the docking of the compounds at the GABA-site appears to require an interaction with the NH_2-terminal variable portion of loop-F of the α–subunit thus achieving a significant degree of isoform selectivity.

2. Materials and methods

2.1. Compounds

All experimental compounds (Fig. 1) were synthesized at Egis Pharmaceuticals PLC as previously described (Ling et al., 2015), and were used at 95% purity or greater. All chemical and biochemical reagents were of the highest grade available. For all *in vitro* experiments a stock solution of the drug (10 mM) was dissolved in 100% DMSO aliquoted and stored at −20 °C. In the *in vitro* assays 0.1% DMSO had no effect on the various control recordings made. For *in vivo* administration, drugs were dissolved in DMSO and diluted further in 0.4%(w/v) hydroxypropyl methylcellulose suspension (Methocell F4 M, Dow Chemical Company, USA) on the day of testing to achieve a final concentration of DMSO of 1% (v/v).

2.2. Cell culture

Stable human embryonic kidney cell (HEK293) lines obtained upon transfection with cDNAs encoding human α-subunit isoforms as well as with cDNA for rat β2 (short) and rat γ2 (long) in antibiotic resistance variants of the expression vector pcDNA3.1 (Life Technologies, Inc., Carlsbad, CA, USA) or pExchange (Agilent Technologies, Inc., Santa Clara, CA, USA) have been described (Ling et al., 2015). The $GABA_A$ $\alpha_x\beta_2\gamma_2$ cell lines were maintained under triple antibiotic selection using neomycin (0.6 mg/ml), zeocin (0.2 mg/ml) and puromycin (3 μg/ml) in Dulbecco's MEM supplemented with 10 v/v% fetal bovine serum and 10 mM KCl. A further cell line, co-expressing $GABA_A$ β2- and γ2-subunits was propagated under selection with neomycin (0.6 mg/ml), zeocin (0.2 mg/ml), in Dulbecco's MEM supplemented with 10 v/v% fetal bovine serum. These cells were transiently transfected by the calcium-phosphate method (Salmon and Trono, 2006) with the expression vectors of the requisite wild-type and variously mutated α-subunit cDNAs. The cells were collected 48 h later, frozen in a mixture of fetal bovine serum and 10% (v/v) DMSO in aliquots sufficient for seeding a 96-well plate and stored at −150 °C until further use.

2.3. Site-directed mutagenesis

Mutations were introduced by site-directed mutagenesis with custom-designed primers using Phusion High-Fidelity DNA Polymerase (Thermo Fisher Scientific Waltham, MA USA) as per the manufacturer's instructions. The resulting constructs were verified by DNA sequencing of the entire coding region (Biomi Ltd, Gödöllő, Hungary).

2.4. FLIPR dye assay

For fluorescence recordings cells were plated in black, clear-bottom, half-volume 96-well plates coated with poly-*D*-lysine at 50,000 or 100,000 cells per well for stable cell lines and transiently transfected cells, respectively, in 50 μL of growth medium and used 24 h later exactly as reported previously (Ling et al., 2015). Briefly, the cells were washed and incubated at 37 °C in 20 mM HEPES buffered Hank's Balanced Salt Solution (HBSS), pH 7.4 supplemented with FLIPR Membrane Potential Assay Kit BLUE (Molecular Devices, Biberach an der Riß, Germany) dye at 2× dilution. Simultaneously with dye-loading various concentrations of the test compound dissolved in HBSS

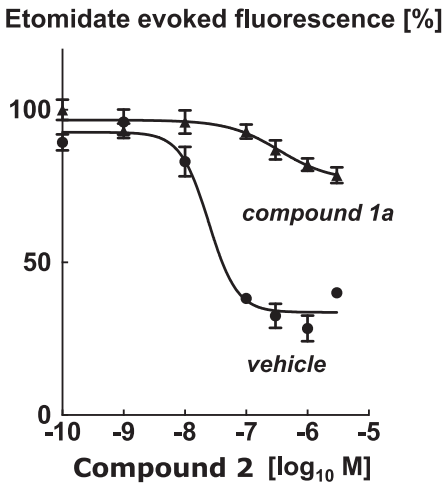

Fig. 2. Inhibition of etomidate-induced depolarization by **2** is blocked by **1a.** HEK293 cells stably expressing α5β2γ2 $GABA_A$Rs, data are means, bars represent S.E.M. n=3. Etomidate concentration was 60 μM (≈EC40), the cells were pretreated for 40 min prior to the introduction of etomidate with various concentrations of **2** (circles) or **2** and **1a** (10 μM, triangles). Representative study from two independent experiments.

supplemented with 20 mM HEPES, pH 7.4 and 1% (v/v) DMSO were added to the incubation medium at 37 °C. The final concentration of DMSO in the medium was 0.1% (v/v). Forty min later the plates were placed into a Flexstation3 (Molecular Devices) plate reader and the recording of fluorescence was started — designated as time 0. Subsequently, the fluorescence signal was sampled at 2 s intervals, the stimulus (GABA or etomidate) was introduced at 30 s, the recording was terminated at 120 s after time 0. Note, that because of the high intracellular concentration of Cl^-, the opening of Cl^- channels in these cells induces depolarization of the membrane potential (Thomas and Smart, 2005) i.e. an increase of the fluorescence signal monitored in this study (Ling et al., 2015). The area under the curve of time *vs.* relative fluorescence units after the addition of GABA was calculated with the average baseline subtracted by Soft-Max 5.4 software (Molecular Devices) and used for further analysis. Non-linear regression curves were fitted using GraphPad Prism version 6.0 and the IC_{50} values to inhibit the effect of GABA were read from the curve. In order to make data comparable between experiments, the results are expressed as percentage of the response evoked by GABA at EC_{20}-EC_{50} depending on the type of the experiment, as specified in the figure legends.

2.5. Homology modelling

The protocol described by Sander and co-workers (Sander et al., 2011) was followed (see Supplement for further details). However, we used the X-ray structure of a ligand *C. elegans* glutamate-gated chloride channel (Hibbs and Gouaux, 2011) as a template. This ligand-bound receptor structure is an invaluable asset for the homology modelling of $GABA_A$ receptors, as none of the templates used previously was a member of this receptor family. The details of the model building, refinement and validation are described in the Supplement. For the sake of comparability we follow the consensus of the corresponding literature in the residue numbering of the subunits. It starts as 9-DNTTV, 7-SNMSL and 22-VPEGD for the subunits α1, β2 and γ2, respectively.

2.6. Novel object preference in mice

Male NMRI mice bred in house were used at 20–30 g body weight. The animals were housed four/cage under standard laboratory conditions (24 ± 2 °C, 40–60% relative humidity), on a 12-h light/dark cycle with light onset at 6:00 AM (Initial Zeitgeber 3). All experimental protocols were approved by the Animal Care and Use Ethical Committee of Egis Pharmaceuticals PLC and complied with the Hungarian Law of Animal Care and Use (1998. XVIII). The test was carried out as previously reported for rats (Gacsályi et al., 2013) with minor modifications. On day 0 (familiarization), the test animals were put in the empty test box (without objects) one by one for 2.5 min each (test box: 24×34×24 cm, black, Plexiglas). The acquisition trial started on day 1 (i.e. 24 h after the end of familiarization; during this time-interval the animals were deprived of food (1 pellet /4 mice) until the end of the acquisition trial). On day 1 (acquisition), each animal was placed in the middle of the test box 60 min after treatment with drug or vehicle. During this trial, mice were allowed to explore two identical objects for 10 s *per* object (within a cut-off time of 5 min). Exploration time was measured manually by stopwatch. After the 5-min acquisition trial, each test animal was returned to its home cage with access to food and water *ad libitum*. The retention trial (on day 2) was started 24 h after the acquisition trial by placing the test animal in the test box containing a replica of the previously explored object and a new object. Exploration times for the two objects were measured during the 4 min retention testing trial. Exclusion criteria: On day 1: exploration time 0 s or extremely low interest (< 1 s) at one object or both objects for the duration of 5 min or the difference of duration of exploration of two objects is > 8 s. On day 2: exploration time 0 s or extremely low interest (< 1 s) at one object or both objects duration of 4 min. Treatment with test compound(s) was by i.p. injection (volume 10 ml/kg) 60 min before the acquisition trial.

3. Results

3.1. Strict requirement for interaction at the GABA binding-site for an inhibitory effect

It was previously demonstrated that **1a** had no appreciable effect on etomidate-induced activation of α5β2γ2 $GABA_A$ Cl^- channels, while **2** was a strong inhibitor (Ling et al., 2015). The data in Fig. 2 show that the inhibitory effect of **2** on depolarization evoked by etomidate was blocked by the prior application of **1a.** Thus similar to bicuculline (Thompson et al., 1999) the effects of **2** are dependent on interaction with the GABA binding-site. Taken together, these findings indicated that binding to the GABA site(s) of the receptor is necessary for an effect on channel gating.

3.2. In silico modelling points to Loop-F as an anchoring point for tricyclic inhibitors

Previously, we reported that the compounds displace ^{3}H-muscimol from the GABA site of α5-$GABA_A$ receptors, whilst having no effect on the binding of the benzodiazepine-site ligand ^{3}H-flumazenil (Ling et al., 2015). In an attempt to understand the mode of interaction of the drugs with the GABA site, *in silico* modelling was used. A homology model of the $\alpha_1\beta_2\gamma_2$ $GABA_AR$ was constructed based on the CLIG homopentameric *C. elegans* glutamate-gated chloride channel (Hibbs and Gouaux, 2011). This particular $GABA_AR$ configuration was chosen because of the wealth of functional of data available on its physiology and pharmacology thus allowing validation of our modell (Krall et al., 2015; Puthenkalam et al., 2016; Sander et al., 2011). Ligand **2** was docked to the refined GABA binding site using the induced-fit docking protocol of the Schrödinger Program Suite (IFD-Schrödinger LLC). Based on the interaction patterns of the 5-(4-piperidyl)-3-isoxazolol and 4-(piperidin-4-yl)-1-hydroxypyrazole derived ligands used by Sander *et al.* (Sander et al., 2011), we selected the binding pose where Arg66 and Arg119 of the α_1-subunit interacted with the oxazolone moiety of the ligand. Loop F of the α_1-subunit was refined using the Prime program (Prime-Schrödinger LLC). The binding position of **2,** together with the schematic map of its interactions, is shown in Fig. 3.

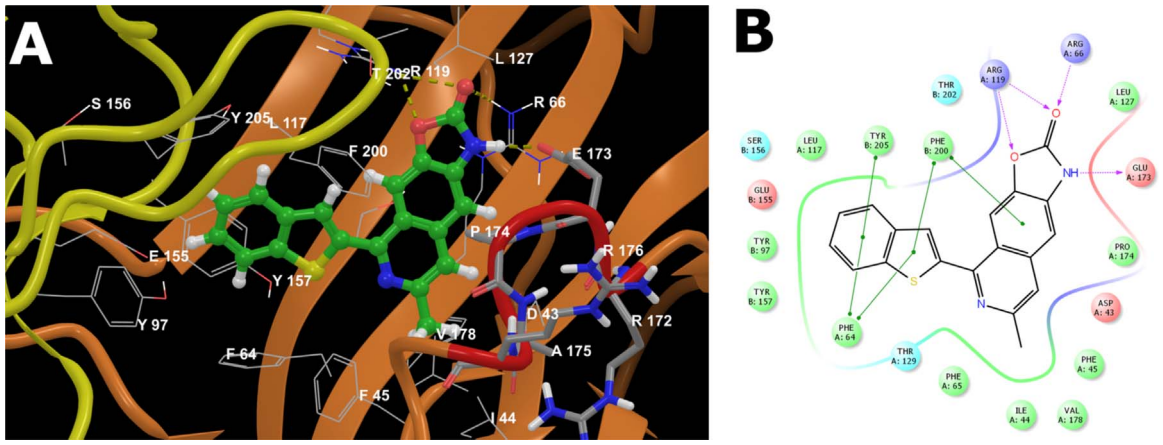

Fig. 3. *In silico* modelling of the interaction of compound **2** with the GABA binding pocket formed at the interface of the α1 and β2 subunits A) The binding position of **2** in the GABA binding pocket of the α1β2γ2 type $GABA_AR$ in close proximity to residues 172–176 (REPAR) from loop F of the α1 subunit, Legend: α1 and β2 subunits are presented in ribbon representation coloured orange and yellow, respectively. Ligand **2** appears in stick and ball representation with green carbon atoms. The bonds of residues 172–176 (REPAR) of subunit α1 are presented as tubes with grey carbon atoms, the corresponding part of the main chain is red. **B**) Interaction map of ligand **2.** H-bonds are represented by magenta arrows, π-π stacking interactions appear as green lines.

As outlined above, the lactone oxygens of the oxazolone moiety were predicted to interact with Arg66 and Arg119, which are known interactors of GABA. Moreover, there was significant proximity of the top of the tricyclic ring with the sequence REPAR mainly in the case of Glu173 and Pro174 of the amino-terminal portion of loop-F of the α1-subunit. The benzothiophene moiety of **2** is found in a hydrophobic pocket formed mainly by Tyr97, Tyr157 and Tyr205 and Phe45, Phe64, Phe200 from the β2- and α1-subunit, respectively. The benzene ring of benzothiophene is situated near Glu155 of the beta subunit, which is a residue also known to be relevant for the interaction with GABA (Newell et al., 2004). The isoquinoline rings were predicted to be surrounded by the hydrophobic residues Ile44, Phe45, Phe65 and Val178 of the α_1-subunit, the latter is also part of loop F. Thus, the docking studies led to the testing of two hypotheses. First, that the orientation of the oxazolone moiety is critical for binding to the GABA site, and second, that the variable NH_2-terminal segment of loop-F of the alpha subunit is also involved.

3.3. Regiochemistry of the oxazolone moiety in vitro and in vivo

Compounds **1c-1** and **1c-2** (Fig. 1) are regiochemical isomers with respect to the positions of N and O in the oxazolone ring. The *in silico* prediction was that the **1c-1** regiochemistry is an absolute requirement for docking in the GABA binding pocket. Indeed, as shown in Fig. 4, 1**c**-1 produced robust inhibition of the GABA response mediated by recombinantly expressed α5β2γ2 $GABA_ARs$ whereas **1c-2** was ineffective up to 100 μM. These results could be also corroborated *in vivo*. Experimental manipulation of α5-$GABA_AR$ function is known influence cognitive performance in rodents (Atack, 2011b; Rudolph and Möhler, 2014). The novel object preference test (Clark, 2013; Kinnavane et al., 2015) in mice, is exquisitely sensitive to compounds influencing α5-$GABA_ARs$ (Ling et al., 2015; Milic et al., 2013; Redrobe et al., 2012). In concordance with the findings on recombinant receptors, compound 1c-1 showed the behavioural effect expected of an inhibitor of α5-$GABA_ARs$: it significantly improved the exploration of the novel object at 10 mg/kg, *i.p.*. In contrast, compound 1c-2 was without significant effect, in agreement with its lack of α5-$GABA_AR$ antagonist efficacy *in vitro* (Fig. 5).

3.4. Role for loop-F of the α-subunits in the inhibitory action of novel tricyclic α5-$GABA_A$ antagonists

Alignment of the primary sequences of the $GABA_A$ α-subunits reveals significant non-homology of the NH_2- terminal portion of

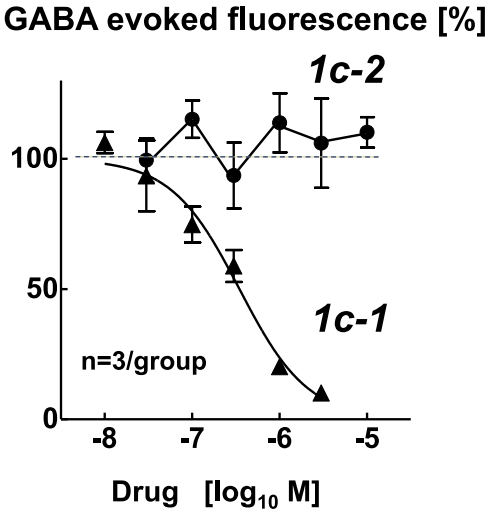

Fig. 4. Strict requirement for the regiochemistry of the oxazolone ring *in vitro*. HEK293 cells stably expressing α5β2γ2 $GABA_ARs$ stimulated with 1.6 μM GABA (≈EC_{40}), data are mean ± S.E.M. n=3/group. Cells were pre-treated for 40 min prior to the introduction of GABA with various concentrations of **1c-2** (circles) or **1c-1** (triangles). Representative study from two independent experiments.

loop-F between the subunit paralogs (Supplementary Fig. 5). Moreover, most of the novel tricyclic inhibitors tested showed a close to 100-fold selectivity for α_5-$GABA_ARs$ over α_2-$GABA_ARs$ (Ling et al., 2015). Thus, α5 "microchimeras" were prepared with sequence modifications derived from the NH_2-terminal segment of loop-F of the α2-(α5-LFα2) and α1-subunits (α5_LFα1), respectively (Fig. 6 and Supplement Fig. 5). Testing of **1b** and **2** on α5-LFα2 subunits revealed a marked reduction of inhibitory potency which was quantifiable for compound **2**: a reduction of 55-fold to 1.6 μM (Fig. 7). In the case of **1b** the lack of a full inhibition of the GABA-induced response on α5-LFα2-$GABA_ARs$ precluded a valid comparison (Fig. 7.). In contrast, only a relatively modest right-shift was found for compound **1a**. By comparison, **2** had an IC_{50} of 993 nM (geometric mean 95% confidence interval=795–1240, n=4) on wild-type α2β2γ2 receptors, while there was no readily quantifiable effect of **1a** or **1b** at up to 10 μM. In the case of **2,** alanine scan of the core loop-F sequence NGSTK revealed that with the exception of asparagine the mutation of all positions to alanine caused a statistically significant diminution of the IC_{50} of **2** (Fig. 8.). The greatest effect was produced by R176A, which caused a close to ten-fold reduction in potency. However, none of the point

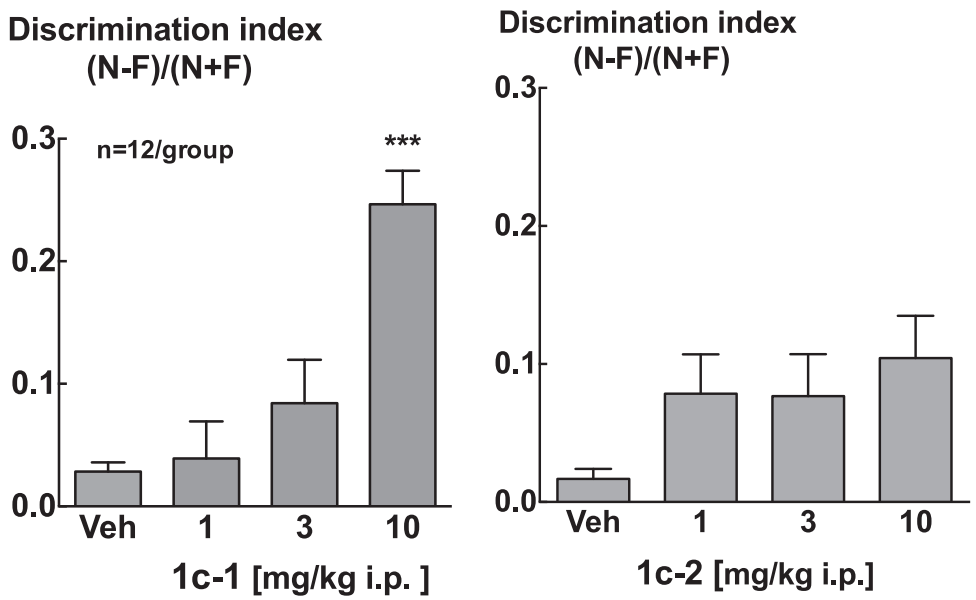

Fig. 5. Strict requirement for the regiochemistry of the oxazolone ring *in vivo*. Object recognition assay in NMRI mice after treatment with vehicle or 1, 3 and 10 mg/kg, *i.p.* of 1c-1 (left) or 1c-2 (right). Data are mean ± S.E.M. n=10/group. The animals were allowed 10 s *per* object contact time (within a cut-off time of 5 min) in the acquisition phase. The test trial took place 24 h later and lasted 4 min. N=time spent in contact with novel object, F=time spent in contact with the familiar object. Animals were injected i.p. with vehicle or the indicated dose of the compounds 60 min prior to the acquisition trial.

mutations approached the reduction in potency seen with the α5-LFα2 construct.

With respect to receptors containing the α5_LFα1 subunit, inhibition by **1b** appeared to fully recapitulate the features of its action on wild-type α1β2γ2 $GABA_A$Rs (Fig. 9). When given alone, **1b** had no effect on the fluorescence signal at concentrations up to 3 μM. In contrast, the characteristics of **2** to inhibit α5_LFα1 receptors were not different from that on α5 receptors (data not shown).

4. Discussion

The results of the present study confirm and extend the finding that the novel tricyclic $GABA_A$ inhibitors have pharmacologic properties similar to bicuculline (Ling et al., 2015; Thompson et al., 1999; Ueno et al., 1997). Interaction of the drugs with the GABA binding-pocket of the $GABA_A$ receptor is essential for biologic efficacy, which has two components. First, competitive inhibition of GABA and second, inhibition of Cl^--channel gating, which becomes apparent when etomidate, a positive allosteric mediator with respect to GABA, is the stimulus. However, some of the compounds (e.g. **1a**) show no discernible effect on channel gating. Importantly, considerable $GABA_A$ α-subunit selectivity (Ling et al., 2015) is evident for oxazolo-2,3,benzodiazepines such as **1b**, which is potentially exploitable for clinical therapy.

The α1β2γ2 $GABA_A$R homology model reported in the present study was largely compiled according to the procedure of Sandberg et al. (Sander et al., 2011) and gave satisfactory docking results for the same set of GABA analogs as tested by these workers. With respect to the docking of the novel tricyclic inhibitors in the GABA binding pocket, the *in silico* modell provided two significant and testable hypotheses. The first concerned the orientation of the oxazolone moiety in the binding pocket (Fig. 4b.). The required regiochemistry with respect to the position of O and N in the oxazolone ring was experimentally validated *in vitro* as well as *in vivo*, thus supporting the notion regarding the orientation of the compounds in the L-shaped

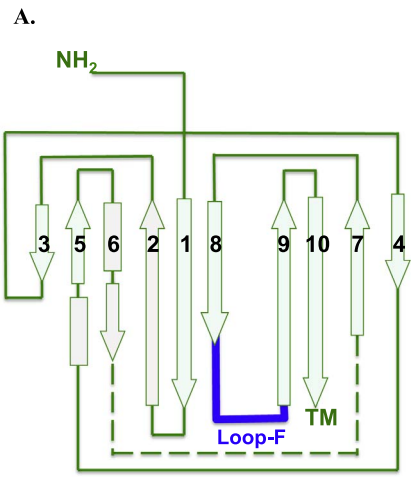

B.

α5_WT VVYVWTNGSTKSVVVAEDG
α5_LF1 VVYEWTREPARSVVVAEDG
α5_LF2 VTYVWTYNASDSVVVAPDG

Fig. 6. A. Schematic representation of the extracellular N-terminal domain of a $GABA_A$ receptor subunit with the relative positions of the beta-sheets (numbered) indicated (Ernst et al., 2005). Ribbons indicate beta-sheets, the arrowheads point towards the carboxyl-terminus. Lines show the connecting loops, Loop-F is highlighted in blue. TM – beginning of the first transmembrane domain. B. The mutations introduced into loop-F of the $GABA_A$ α5-subunit – derived from homologous sections of the α1 and α2 subunits, respectively (Also see Supplementary Fig. 5).

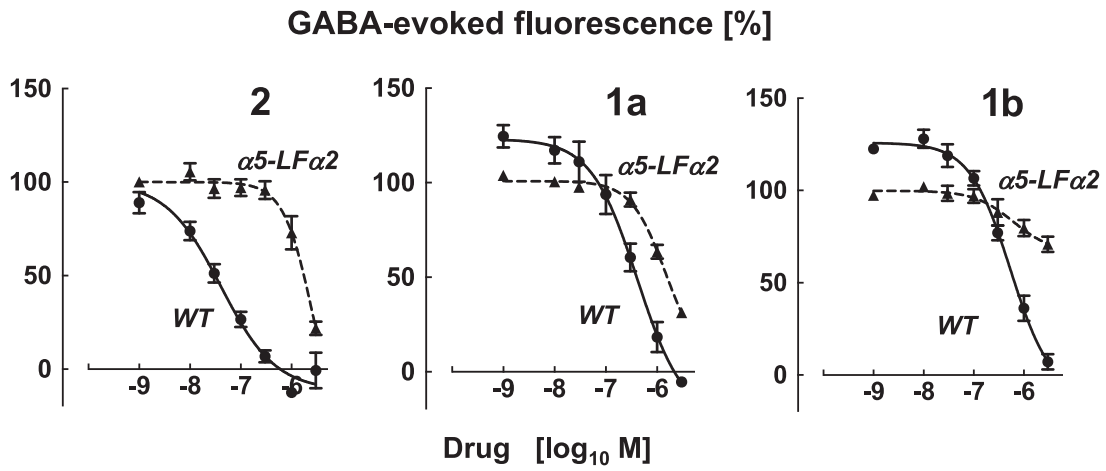

Fig. 7. Effects of introducing mutations derived from the $GABA_A$ α_2-subunit into loop-F of the $GABA_A$ α_5 subunit on the potencies of compounds **2**, **1a** and **1b** to inhibit the depolarization evoked by 0.4 μM GABA (≈EC_{60} for both receptors). HEK293 cells stably expressing β2γ2 subunits and transiently transfected with α5 (circles) or α5_LFα2 (triangles) subunit cDNA. Data are mean ± S.E.M. n=3/group. Representative study from two independent experiments.

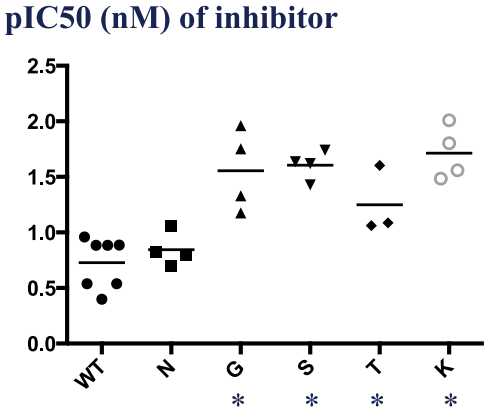

Fig. 8. Alanine-scan of loop-F with respect to the inhibitory action of compound **2** on α5β2γ2 $GABA_AR$ transiently expressed in HEK293 cells. In each case the pIC_{50} value was determined against 0.8 μM GABA ≈$EC_{20–50}$ as the stimulus, the pIC_{50} value was calculated by non-linear regression using Graph-Pad Prism four-parameter curve-fitting. The results of individual experiments are shown, horizontal bars represent the mean. Wild type (WT), single letter amino acid code is used on the x-axis to indicate which amino acid was mutated to A. One-way ANOVA, followed by Dunnett's test for multiple comparisons, * $P < 0.05$, ** $P < 0.01$ when compared to from WT.

binding pocket.

Second, given the orientation of the oxazolone moiety, the model indicated that the $GABA_AR$ isoform selectivity of the test compounds could be derived from interactions with the variable NH_2-terminal segment of the loop-F of the α-subunit. Loop-F (called loop 9 in some studies) connects beta-sheets 8 and 9 of the extracellular domain of $GABA_ARs$ (Fig. 7A). Loop-F has no known structure (Bergmann et al., 2013; Miller and Aricescu, 2014) and its functional role in $GABA_AR$ is not fully understood (Khatri and Weiss, 2010; Lynagh and Pless, 2014). High-resolution structural analyses (Miller and Aricescu, 2014; Spurny et al., 2012) indicated that while loop-F is in close proximity of the GABA binding-pocket, it is not part of it. In contrast, homology-based computer modelling indicated that the lower, carboxyl-terminal domain of loop-F, including Val178 and Val180, faces the GABA binding-pocket (Bergmann et al., 2013; Newell and Czajkowski, 2003; Puthenkalam et al., 2016; Sander et al., 2011). Moreover, *N*-Biotinylaminoethyl methanethiosulfonate labelling implicated R176, Val178 and Val180 in the action of GABA (Newell and Czajkowski, 2003). However, point mutations to cysteine in loop-F the α-subunit of α1-$GABA_AR$ had no significant effect on GABA potency (Newell and Czajkowski, 2003). It is well documented that loop-F undergoes marked conformation changes upon the binding of GABA in GABA-C receptors (Khatri et al., 2009; Zhang et al., 2009). Similar findings were reported upon proton activation of the prokaryotic channel GLIC (Dellisanti et al., 2013). Analysis of molecular dynamic simulations of a homology model of heteropentameric receptors with GABA α1 or α6 subunits indicated that loop-F regulates the affinity for GABA in a subunit-specific manner (Carpenter et al., 2012). Taken together, in $GABA_ARs$ the role of loop-F of the α-subunit is controversial with respect to the binding and recognition of agonists. More pertinent for the present study are the reports showing that the potency of the competitive antagonists *d*-tubocurarine and strychnine on the CLIG-family member 5-HT_3, nicotinic as well as glycine receptors is strongly dependent on the sequence of loop-F (Dutzler et al., 2011; Zhang et al., 2007). However, in contrast to $GABA_ARs$, it is well established that loop-F contributes to the agonist binding-pocket of these receptors (Lynagh and Pless, 2014).

The present study found that the three novel analogs tested on recombinantly expressed α5_LFα2β2γ2 $GABA_ARs$ displayed different changes in potency. Compounds **2** and **1b** had characteristics closely resembling those on recombinantly expressed wild-type α2β2γ2 $GABA_ARs$. By contrast, in the case of compound **1a** only a minor right-shift of the concentration-response curve was observed, whereas this compound was without quantifiable effect on wild type α2β2γ2 $GABA_ARs$. With respect to α5_LFα1β2γ2 $GABA_ARs$, the pattern of inhibition by compound **1b** closely resembled that seen in α1β2γ2 $GABA_ARs$. In contrast, the potency and maximal effect of **2** remained unaltered, i.e. retaining roughly 10-fold selectivity towards α5β2γ2 $GABA_ARs$ over α1β2γ2 $GABA_ARs$ (Ling et al., 2015). These data indicate that the contribution of loop-F to the potencies of the test compounds may vary with the compound tested as well as with the α-subunit investigated. Thus these compounds may prove useful to explore the various conformations of loop-F of the α-subunits. Intriguingly, **1b,** a compound with drug-like properties that appeared to be selective for extrasynaptic α5-$GABA_ARs$ (Ling et al., 2015), showed the most marked and consistent loop-F dependence.

Alanine-scan of the NGSTK sequence in α5-$GABA_ARs$ indicated contributions of all residues apart from N173 to the potency of **2**, with residue K176 causing the largest right-shift of about 10-fold. By comparison, the potency of **2** on receptors containing microchimeric α5_LF2 subunits was reduced by over 50-fold. Taken together, the results indicate that it is the ensemble of loop-F stretching from residues 169 to 182 that is required for the high-affinity binding of the test compounds to the GABA binding-pocket. Given the structural flexibility of loop-F and the localized sequence variability at positions 173–177, a wide spectrum of receptor-drug conformers is likely to contribute to the macroscopic characteristics of the cellular response to

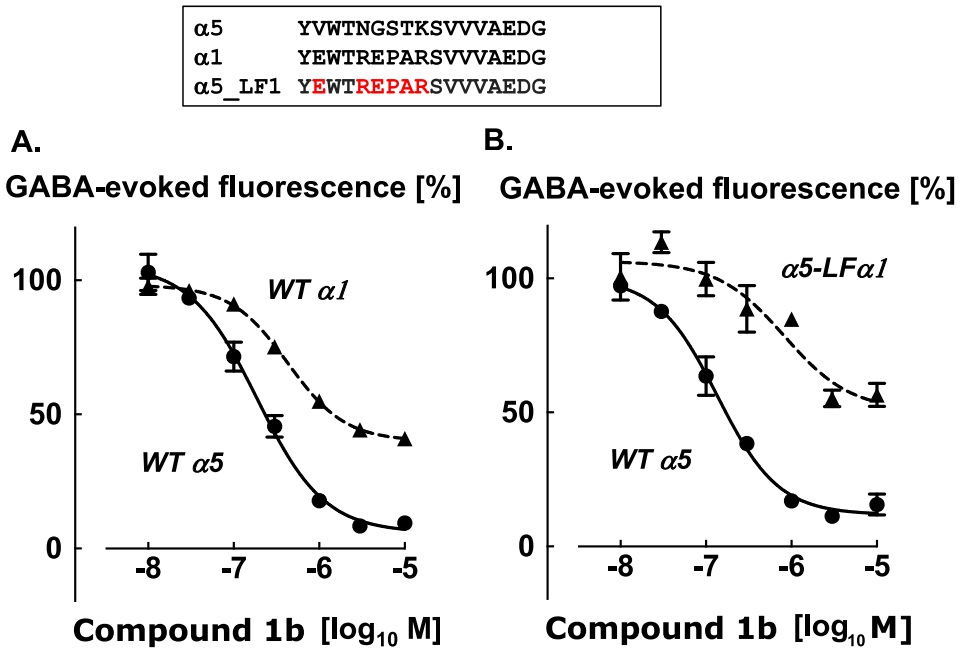

Fig. 9. Characteristics of the inhibition α1-$GABA_A$Rs by **1b** apparent in receptors comprised of α5_LFα1 microchimeric α-subunits. Left panel; HEK293 cells stably expressing α5β2γ2 (WT α5, circles) or α1β2γ2 $GABA_A$Rs (WT α1, triangles). Right panel: HEK 293 cells stably expressing β2γ2 subunits, transiently transfected with wild type α5 (WT α5, circles) or α5_LFα1 (triangles) subunit cDNA. GABA was used at 1.6 μM – between EC_{20} and EC_{50} for the various receptor configurations. The inset shows the single letter amino acid sequence, changes introduced into α5_LFα1 are highlighted in red.

the novel tricyclic $GABA_A$ antagonist compounds.

5. Conclusion

The data presented here conform to the hypothesis that the novel tricyclic α5-$GABA_A$ antagonist compounds bind to the GABA site(s) of $GABA_A$ hetero-pentameric receptors. Binding of the compounds at the GABA-site is dependent on an interaction with the NH_2-terminal segment of loop-F of the alpha subunit. As this part of the protein shows marked sequence variability between the alpha subunit paralogs, the interaction with loop-F imparts a significant degree of $GABA_A$ receptor subtype selectivity to the novel antagonists. A member of this class of compounds is now in Phase 2 clinical trials (https://www.clinicaltrialsregister.eu/ctr-search/trial/2016-001005-16/HU).

Acknowledgements

With the exception of FB[c], FB[d] and TM all authors were employees of Egis Pharmaceuticals PLC, Budapest, Hungary. The work of TM is supported by the Lendület (Momentum) program of the Hungarian Academy of Sciences. We thank Dr. Patricia Machado (Les Laboratoires Servier, Suresnes, France) for helpful comments on the manuscript.

Appendix A. Supporting information

Supplementary data associated with this article can be found in the online version at doi:10.1016/j.ejphar.2017.01.033.

References

Araujo, F., Ruano, D., Vitorica, J., 1999. Native gamma-aminobutyric acid type A receptors from rat hippocampus, containing both alpha 1 and alpha 5 subunits, exhibit a single benzodiazepine binding site with alpha 5 pharmacological properties. J. Pharmacol. Exp. Ther. 290, 989–997.

Atack, J.R., 2011a. $GABA_A$ receptor subtype-selective modulators. I. alpha2/alpha3-selective agonists as non-sedating anxiolytics. Curr. Top. Med. Chem. 11, 1176–1202.

Atack, J.R., 2011b. $GABA_A$ receptor subtype-selective modulators. II. alpha5-selective inverse agonists for cognition enhancement. Curr. Top. Med. Chem. 11, 1203–1214.

Barnard, E.A., Darlison, M.G., Fujita, N., Glencorse, T.A., Levitan, E.S., Reale, V., Schofield, P.R., Seeburg, P.H., Squire, M.D., Stephenson, F.A., 1988. Molecular biology of the $GABA_A$ receptor. Adv. Exp. Med. Biol. 236, 31–45.

Bergmann, R., Kongsbak, K., Sorensen, P.L., Sander, T., Balle, T., 2013. A unified model of the GABA(A) receptor comprising agonist and benzodiazepine binding sites. PLoS One 8, e52323.

Carpenter, T.S., Lau, E.Y., Lightstone, F.C., 2012. A role for loop F in modulating GABA binding affinity in the GABA(A) receptor. J. Mol. Biol. 422, 310–323.

Clark, R.E., 2013. Recognition memory: an old idea given new life. Curr. Biol. 23, R725–R727.

Dellisanti, C.D., Ghosh, B., Hanson, S.M., Raspanti, J.M., Grant, V.A., Diarra, G.M., Schuh, A.M., Satyshur, K., Klug, C.S., Czajkowski, C., 2013. Site-directed spin labeling reveals pentameric ligand-gated ion channel gating motions. PLoS Biol. 11, e1001714.

Dutzler, R., Brams, M., Pandya, A., Kuzmin, D., van Elk, R., Krijnen, L., Yakel, J.L., Tsetlin, V., Smit, A.B., Ulens, C., 2011. A structural and mutagenic blueprint for molecular recognition of strychnine and d-tubocurarine by different Cys-loop receptors. PLoS Biol. 9, e1001034.

Ernst, M., Bruckner, S., Boresch, S., Sieghart, W., 2005. Comparative models of $GABA_A$ receptor extracellular and transmembrane domains: important insights in pharmacology and function. Mol. Pharmacol. 68, 1291–1300.

Gacsályi, I., Nagy, K., Pallagi, K., Lévay, G., Hársing, L.G., Jr., Móricz, K., Kertész, S., Varga, P., Haller, J., Gigler, G., Szénási, G., Barkóczy, J., Biró, J., Spedding, M., Antoni, F.A., 2013. Egis-11150: a candidate antipsychotic compound with procognitive efficacy in rodents. Neuropharmacology 64, 254–263.

Hibbs, R.E., Gouaux, E., 2011. Principles of activation and permeation in an anion-selective Cys-loop receptor. Nature 474, 54–60.

IFD-Schrödinger LLC, Schrödinger Suite 2014-1, Induced Fit Docking protocol. New York.

Khatri, A., Sedelnikova, A., Weiss, D.S., 2009. Structural rearrangements in loop F of the GABA receptor signal ligand binding, not channel activation. Biophys. J. 96, 45–55.

Khatri, A., Weiss, D.S., 2010. The role of Loop F in the activation of the GABA receptor. J. Physiol. 588, 59–66.

Kinnavane, L., Albasser, M.M., Aggleton, J.P., 2015. Advances in the behavioural testing and network imaging of rodent recognition memory. Behav. Brain Res. 285, 67–78.

Klausberger, T., Somogyi, P., 2008. Neuronal diversity and temporal dynamics: the unity of hippocampal circuit operations. Science 321, 53–57.

Krall, J., Balle, T., Krogsgaard-Larsen, N., Sorensen, T.E., Krogsgaard-Larsen, P., Kristiansen, U., Frølund, B., 2015. $GABA_A$ receptor partial agonists and antagonists: structure, binding mode, and pharmacology. Adv. Pharmacol. 72, 201–227.

Ling, I., Mihalik, B., Etherington, L.A., Kapus, G., Pálvölgyi, A., Gigler, G., Kertész, S., Gaál, A., Pallagi, K., Kiricsi, P., Szabó, E., Szénási, G., Papp, L., Hársing, L.G., Lévay, G., Spedding, M., Lambert, J.J., Belelli, D., Barkóczy, J., Volk, B., Simig, G., Gacsályi, I., Antoni, F.A., 2015. A novel GABA(A) alpha 5 receptor inhibitor with therapeutic potential. Eur. J. Pharmacol. 764, 497–507.

Lynagh, T., Pless, S.A., 2014. Principles of agonist recognition in Cys-loop receptors. Front. Physiol. 5, 160.

McKernan, R.M., Whiting, P.J., 1996. Which $GABA_A$-receptor subtypes really occur in

the brain? Trends Neurosci. 19, 139–143.
Milic, M., Timic, T., Joksimovic, S., Biawat, P., Rallapalli, S., Divljakovic, J., Radulovic, T., Cook, J.M., Savic, M.M., 2013. PWZ-029, an inverse agonist selective for alpha(5) $GABA_A$receptors, improves object recognition, but not water-maze memory in normal and scopolamine-treated rats. Behav. Brain Res. 241, 206–213.
Miller, P.S., Aricescu, A.R., 2014. Crystal structure of a human $GABA_A$ receptor. Nature 512, 270–275.
Miller, P.S., Smart, T.G., 2010. Binding, activation and modulation of Cys-loop receptors. Trends Pharmacol. Sci. 31, 161–174.
Newell, J.G., Czajkowski, C., 2003. The $GABA_A$ receptor alpha 1 subunit Pro174-Asp191 segment is involved in GABA binding and channel gating. J. Biol. Chem. 278, 13166–13172.
Newell, J.G., McDevitt, R.A., Czajkowski, C., 2004. Mutation of glutamate 155 of the $GABA_A$ receptor beta2 subunit produces a spontaneously open channel: a trigger for channel activation. J. Neurosci. 24, 11226–11235.
Nusser, Z., Sieghart, W., Somogyi, P., 1998. Segregation of different GABAA receptors to synaptic and extrasynaptic membranes of cerebellar granule cells. J. Neurosci. 18, 1693–1703.
Olsen, R.W., Sieghart, W., 2008. International Union of Pharmacology. LXX. Subtypes of gamma-aminobutyric acid(A) receptors: classification on the basis of subunit composition, pharmacology, and function. Update. Pharmacol. Rev. 60, 243–260.
Pollard, S., Thompson, C.L., Stephenson, F.A., 1995. Quantitative characterization of alpha 6 and alpha 1 alpha 6 subunit-containing native gamma-aminobutyric acidA receptors of adult rat cerebellum demonstrates two alpha subunits per receptor oligomer. J. Biol. Chem. 270, 21285–21290.
Prime-Schrödinger LLC, Schrödinger Suite 2014-1, Prime. New York.
Puthenkalam, R., Hieckel, M., Simeone, X., Suwattanasophon, C., Feldbauer, R.V., Ecker, G.F., Ernst, M., 2016. Structural studies of $GABA_A$ receptor binding sites: which experimental structure tells us what? Front. Mol. Neurosci. 9, 44.
Redrobe, J.P., Elster, L., Frederiksen, K., Bundgaard, C., de Jong, I.E., Smith, G.P., Bruun, A.T., Larsen, P.H., Didriksen, M., 2012. Negative modulation of $GABA_A$ alpha5 receptors by RO4938581 attenuates discrete sub-chronic and early postnatal phencyclidine (PCP)-induced cognitive deficits in rats. Psychopharmacology 221, 451–468.
Rudolph, U., Möhler, H., 2014. $GABA_A$ receptor subtypes: therapeutic potential in Down syndrome, affective disorders, schizophrenia, and autism. Annu. Rev. Pharmacol. Toxicol. 54, 483–507.
Salmon, P., Trono, D., 2006. Production and titration of lentiviral vectors. Curr. Protoc. Neurosci., (Chapter 4, Unit 4 21).
Sander, T., Frølund, B., Bruun, A.T., Ivanov, I., McCammon, J.A., Balle, T., 2011. New insights into the GABA(A) receptor structure and orthosteric ligand binding: receptor modeling guided by experimental data. Proteins-Struct. Funct. Bioinform. 79, 1458–1477.
Skolnick, P., 2012. Anxioselective anxiolytics: on a quest for the Holy Grail. Trends Pharmacol. Sci. 33, 611–620.
Spurny, R., Ramerstorfer, J., Price, K., Brams, M., Ernst, M., Nury, H., Verheij, M., Legrand, P., Bertrand, D., Bertrand, S., Dougherty, D.A., de Esch, I.J., Corringer, P.J., Sieghart, W., Lummis, S.C., Ulens, C., 2012. Pentameric ligand-gated ion channel ELIC is activated by GABA and modulated by benzodiazepines. Proc. Natl. Acad. Sci. USA 109, E3028–E3034.
Thomas, P., Smart, T.G., 2005. HEK293 cell line: a vehicle for the expression of recombinant proteins. J. Pharmacol. Toxicol. Methods 51, 187–200.
Thompson, S.A., Smith, M.Z., Wingrove, P.B., Whiting, P.J., Wafford, K.A., 1999. Mutation at the putative GABA(A) ion-channel gate reveals changes in allosteric modulation. Br. J. Pharmacol. 127, 1349–1358.
Ueno, S., Bracamontes, J., Zorumski, C., Weiss, D.S., Steinbach, J.H., 1997. Bicuculline and gabazine are allosteric inhibitors of channel opening of the $GABA_A$ receptor. J. Neurosci. 17, 625–634.
Walker, J.E., 1983. Glutamate, GABA, and CNS disease: a review. Neurochem. Res. 8, 521–550.
Wikipedia, 2015. Basmisanil.
Zhang, J., Xue, F., Chang, Y., 2009. Agonist- and antagonist-induced conformational changes of loop F and their contributions to the rho1 GABA receptor function. J. Physiol. 587, 139–153.
Zhang, R., Wen, X., Militante, J., Hester, B., Rhubottom, H.E., Sun, H., Leidenheimer, N.J., Yan, D., White, M.M., Machu, T.K., 2007. The role of loop F residues in determining differential d-tubocurarine potencies in mouse and human 5-hydroxytryptamine 3A receptors. Biochemistry 46, 1194–1204.